Shear Alfvén Wave (SAW) Spectra in a Periodic Magnetic Mirror Array

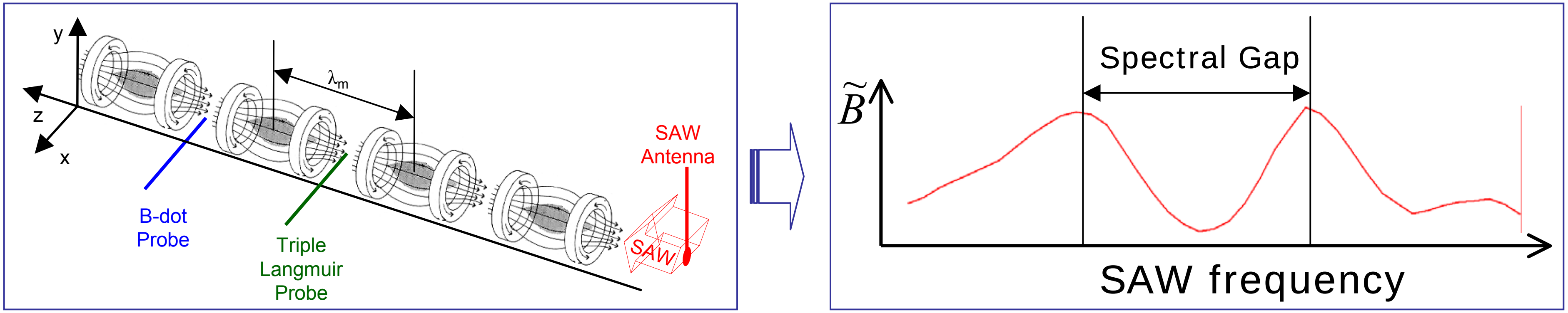

Y. Zhang, W.W. Heidbrink, H. Boehmer, R. McWilliams (UC Irvine)
Guangye Chen, Boris N. Breizman (UT Austin)
S. Vincena, T. Carter, D. Leneman, W. Gekelman, B. Brugman (UCLA)

http://hal9000.ps.uci.edu/Presentations.htm

Work supported by DOE DE-FG02-03ER54720

UCIrvine THE UNIVERSITY OF TEXAS AT AUSTIN UCLA

Periodic Structures Influence Wave Propagation in Many Physical Environments

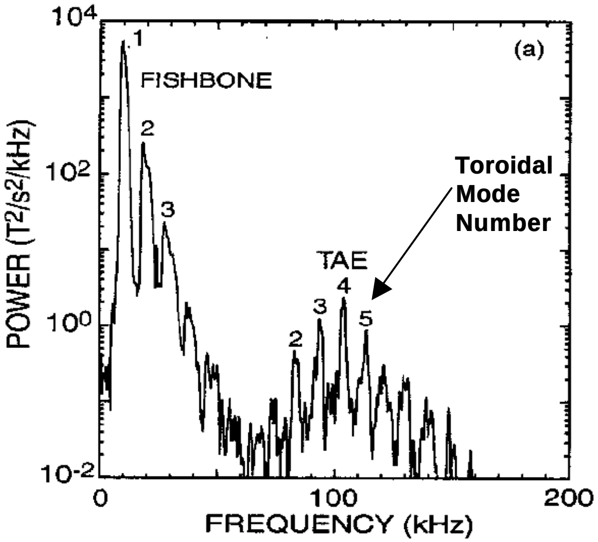

Fig. 1. TAE structure in DIIID
(E. M. Carolipio et. al. PoP 8(7) 3391, 2001)

$\omega_{TAE} \sim v_A / 2qR$, $L = qR$, $q(r_m) \sim m / n$

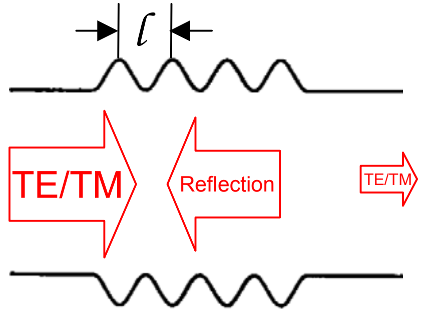

Fig. 2. Waveguide Bragg Reflector

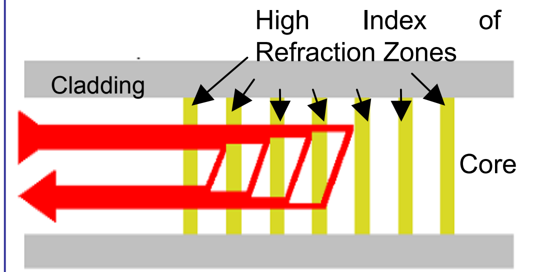

Fig. 3. Optic Fiber Bragg Grating

$\varepsilon = \varepsilon_0 [1 + M \cos(\vec{K} \cdot \vec{r})]$

Waves in a **periodic** medium
(or boundary condition)

?

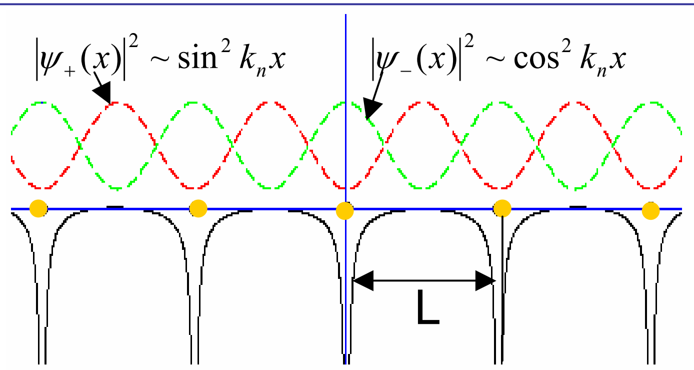

Fig. 4. Solid - state Electron Probability Density in Periodic Ion Core Potential

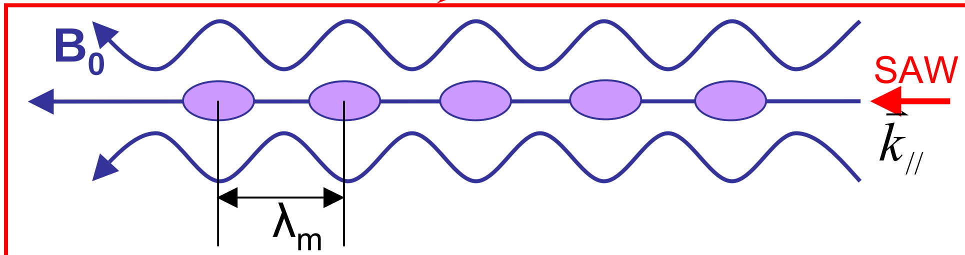

Given Bragg reflection condition $2k_{//} = k_m$ or $\lambda = 2\lambda_m$,
a **propagation gap** is centered at $f_B = v_{A//} / 2\lambda_m$

Fig. 5. Mirror Alfvén Experiment in LAPD

Similarities: TAE and Multiple Mirror Alfvén Experiment

	TAE	Multiple Mirror Alfvén Experiment
Periodicity	Magnetic field: $B_0\,(\theta)$	Magnetic field: $B_0\,(z)$
Periodic length	$2\pi qR$	Mirror cell length: λ_m
Mirror Depth	$\varepsilon = r / R$	$\frac{B_{\max} - B_{\min}}{B_{\max} + B_{\min}}$
Wave function	$\sim exp(im\theta)$	$\sim exp(ik_{//} z)$
Physical quantity	Plasma displacement: $\lvert\xi(\theta)\rvert^2$	SAW field energy: $\lvert\tilde{B}(z)\rvert^2$
Bragg Condition	$k_{//}=n/2qR$	$k_n=n\pi/\lambda_m$
Spectral Gap	☑	☑ Experiment ☑ Simulation
Eigenmodes	☑	?

Mirror Array Configuration in Well Diagnosed LAPD Plasma

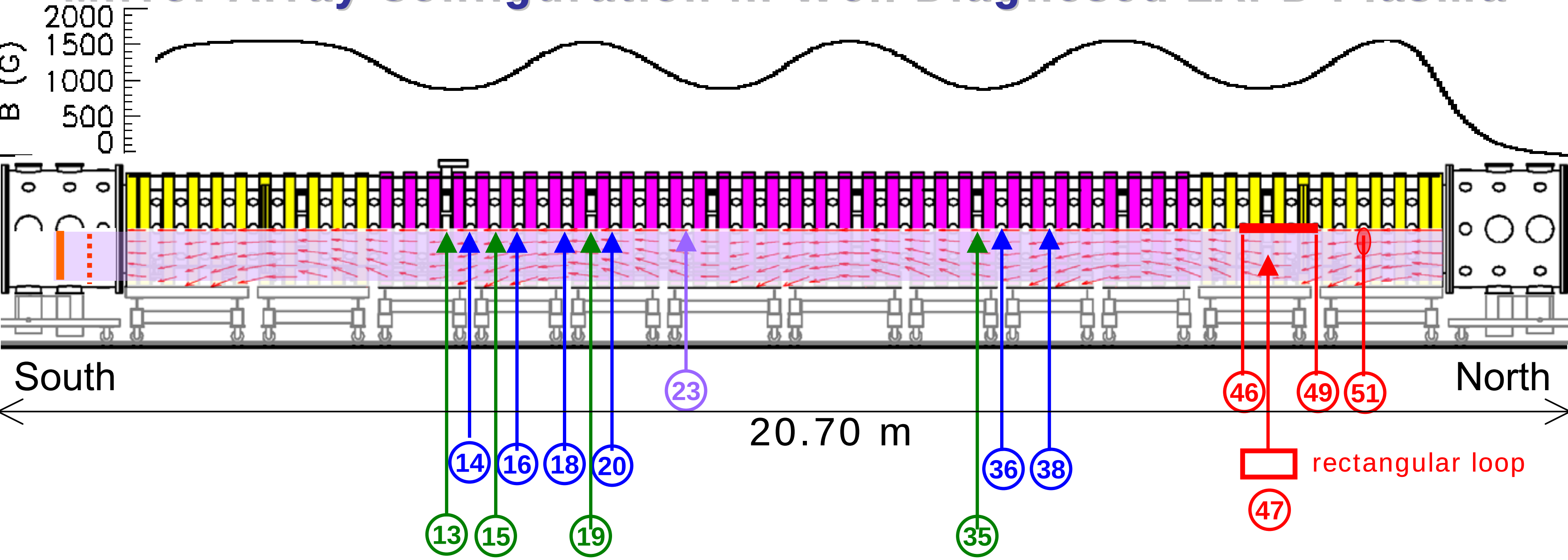

- LAPD chamber length 20.70 m, diameter 1.0 m; Experimental plasma length 16.54 m.
- Various mirror array configurations are powered by 10 independent magnet power supplies; B_0~ 0.5 kG – 2.0 kG.
- Helium plasma column density FWHM ~0.60 m, (1 shot per second cathode discharge)
- Microwave interferometers for column plasma density calibration (port 23) ($n_{peak} \approx 1 \times 10^{12}$ /cm^3)
- Triple probes for local Te, n_i, V_f measurements (port 13, 15, 19, 35)
- SAW antennas: small disk (p51); copper rod (p46 to p49); rectangular loop (p47)
- B-dot probes for local B_{SAW} measurements (port 14, 16, 18, 20, 36, 38)

MIRROR ARRAY ALFVÉN EXPERIMENT (UC IRVINE, UCLA)

- Shear Alfvén Wave (SAW) propagation in a mirror array field
  - Local Alfvén speed (v_A) varies periodically with mirror magnetic field
  - SAW refraction in perpendicular direction
  - Standing wave modes observed at gap frequency—standing wavelength ($\sim\lambda_m/2$) observed
- Alfvén wave field spectral gaps are observed in various mirror configurations:
  - Spectral gap is observed with at least 4 mirror cells in a series
  - Spectral gap width is linearly proportional to mirror depth
  - Spectral gap depth is proportional to mirror depth

UCIrvine

UCLA

Plasma Parameters Vary Between: B_{max} (IAW) and B_{min} (KAW)

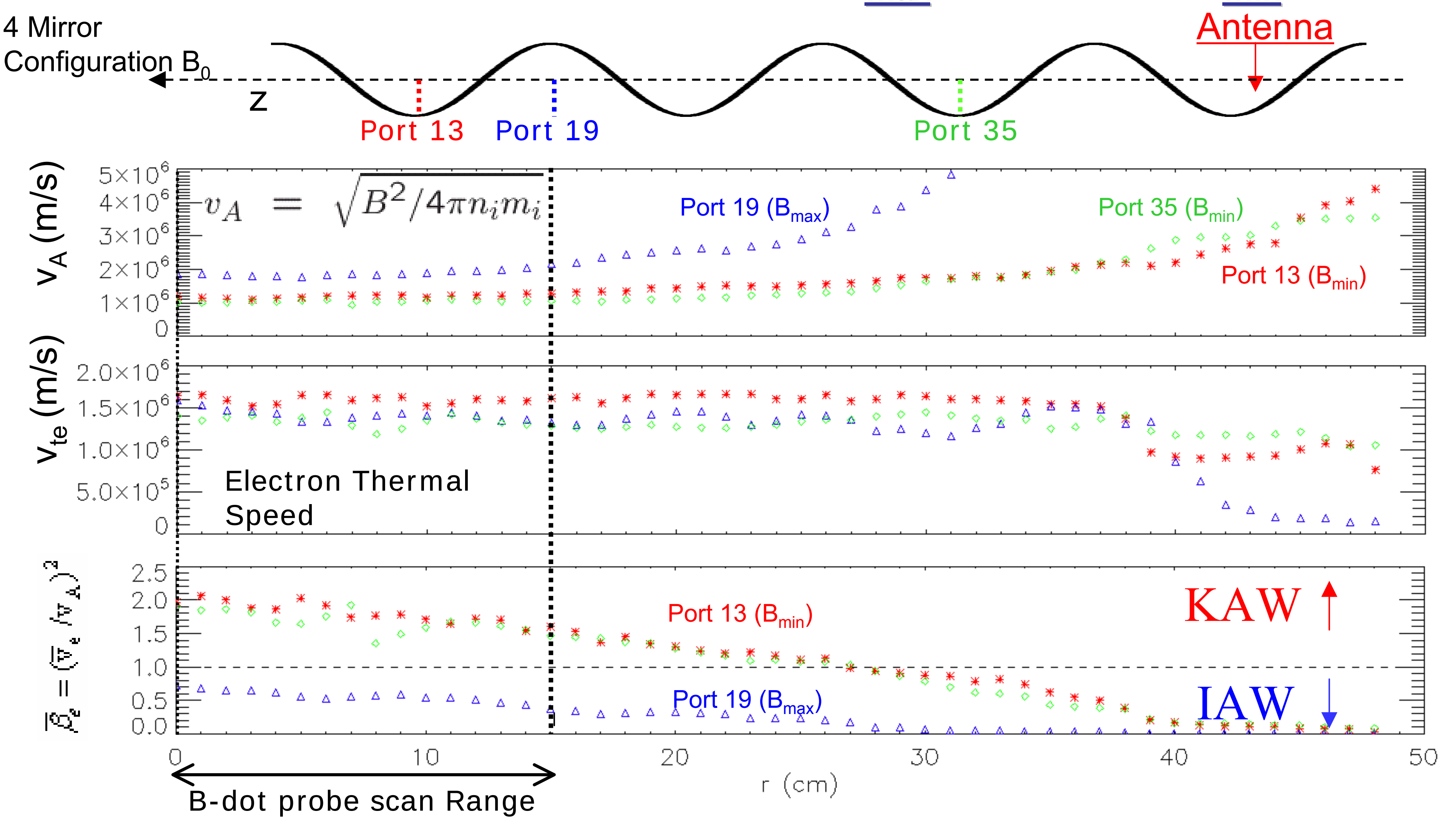

Inertial Alfvén Wave (IAW)—

Electrons respond **inertially** to $E_{//}$ of the wave.

$$\overline{\beta}_e = \beta_e \frac{m_i}{m_e} = (\overline{v}_e/v_A)^2 \ll 1$$

Kinetic Alfvén Wave (KAW)—

Electrons respond **adiabatically** to $E_{//}$ of the wave.

$$\overline{\beta}_e = \beta_e \frac{m_i}{m_e} = (\overline{v}_e/v_A)^2 \gg 1$$

Examples of SAW Antennas and Wave Patterns

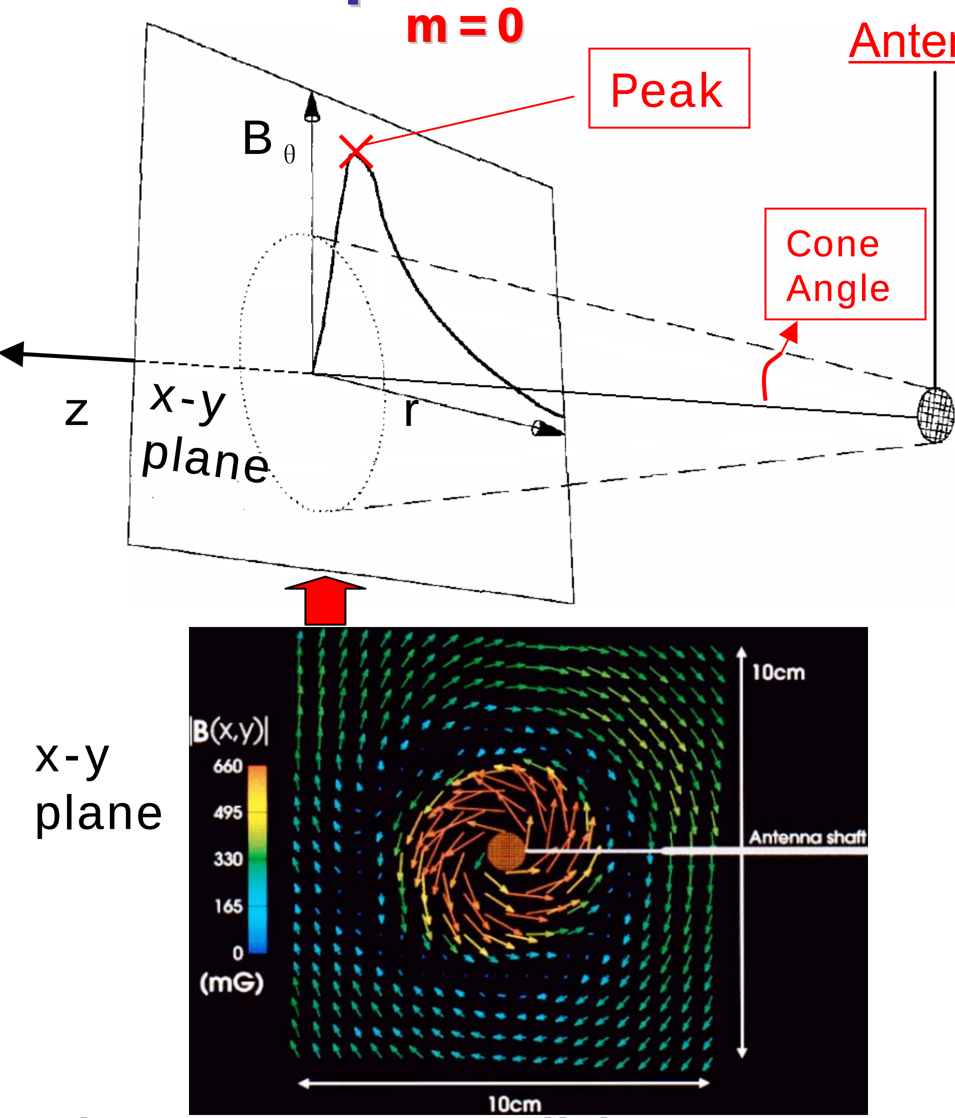

Fig. 1. Dia.=1.0 cm **disk antenna** [1] /
Dia.=0.96 cm, l=96 cm **rod antenna**. [2]

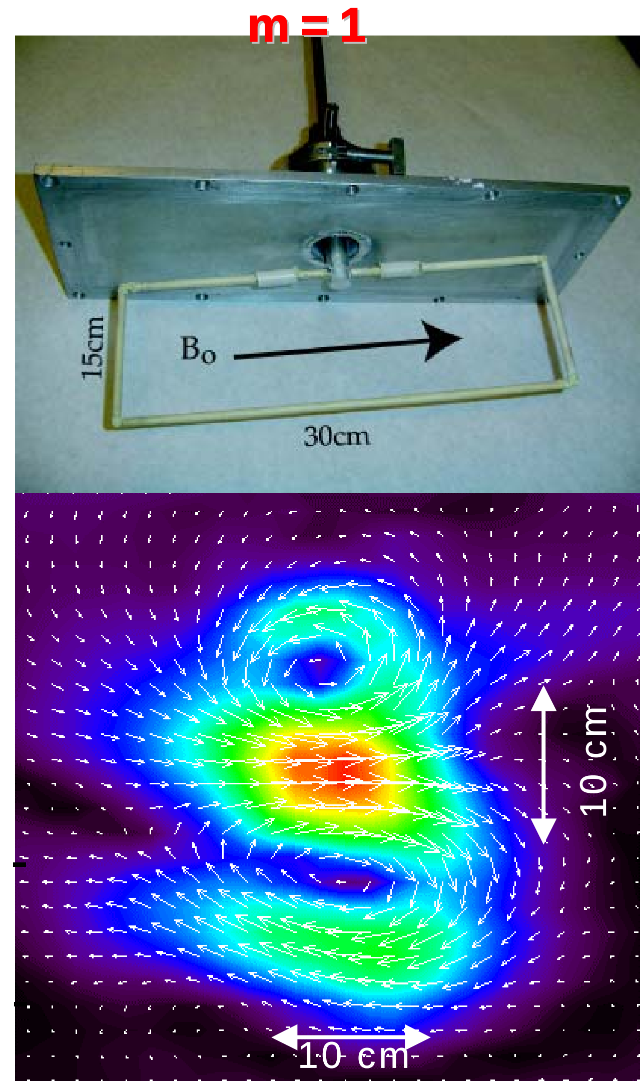

Fig. 2. Rectangular Loop antenna (T. Carter, B. Brugman)

[1] W. Gekelman, D. Leneman, J. Maggs, and S. Vincena, Phys. Plasmas **1** (12), 3775 (1994)
[2] C. C. Mitchell, J. E. Maggs, S. T. Vincena, and W. N. Gekelman, J. Geophys. Res., VOL. 107, NO. A12, 1469 (2002)

Frequency-Spatial SAW Field Scans Show “Cone” Pattern

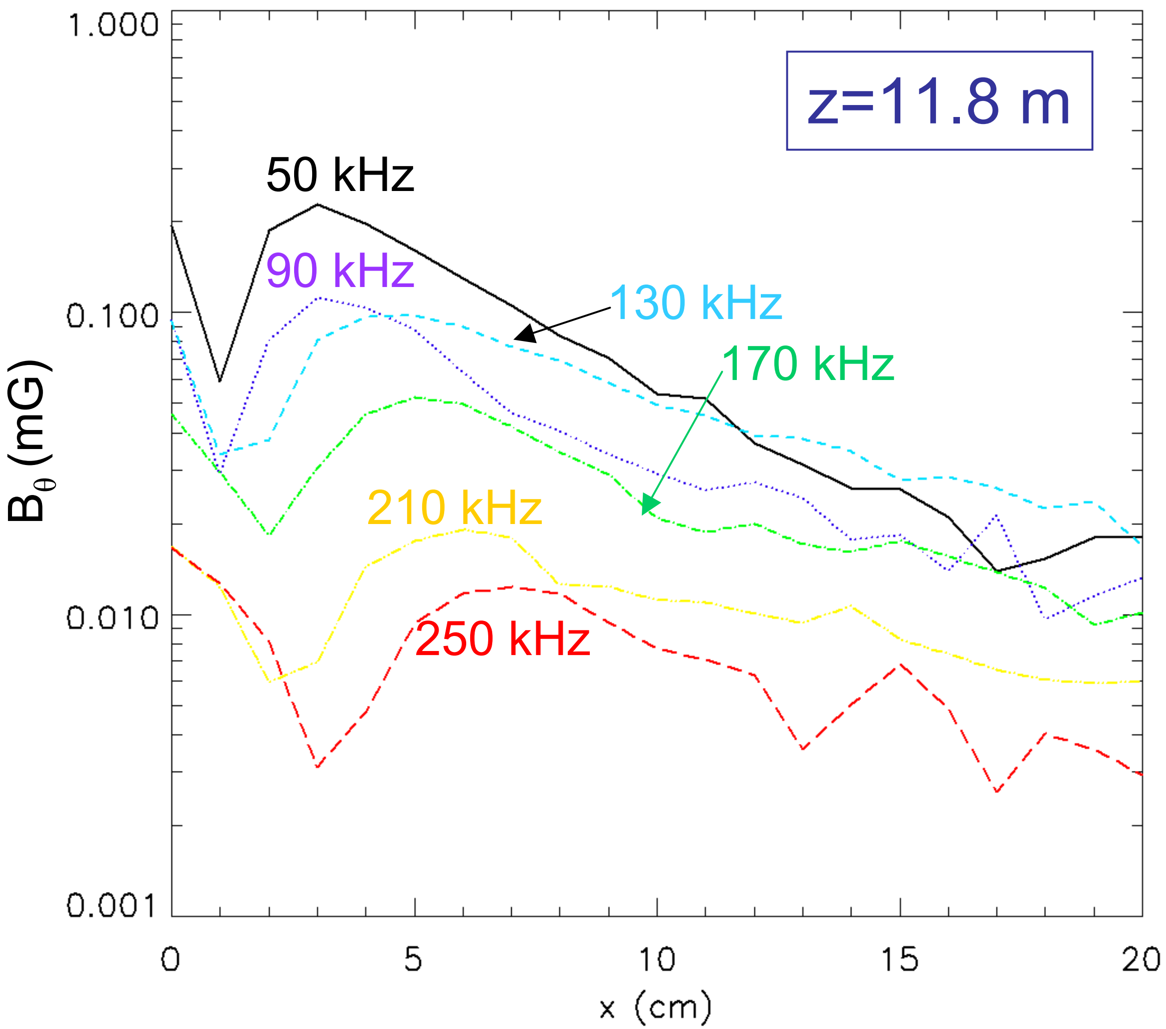

- B-dot probe scans for B_θ (B_y along y=0 line) : 100 MHz maximum sampling rate; 5 to 10 shots averaging at each frequency and each spatial position; 5 kHz frequency scan stepping.

- **Left** figure shows radial profiles for various SAW launching frequencies. (B=1.0 kG)

The spatial profiles resemble the theoretical prediction below:

$$B_\theta(r,z)=\frac{2I_0}{ca}\int_0^\infty dk_\perp \frac{\sin k_\perp a}{k_\perp} J_1(k_\perp r)\exp[ik_\parallel(k_\perp)z]$$

G. J. Morales, R. S. Loritsch, and J. E. Maggs

Phys. Plasmas 1 (12), December 1994 3765

Single Mirror Cell is a Diverging Lens for SAW

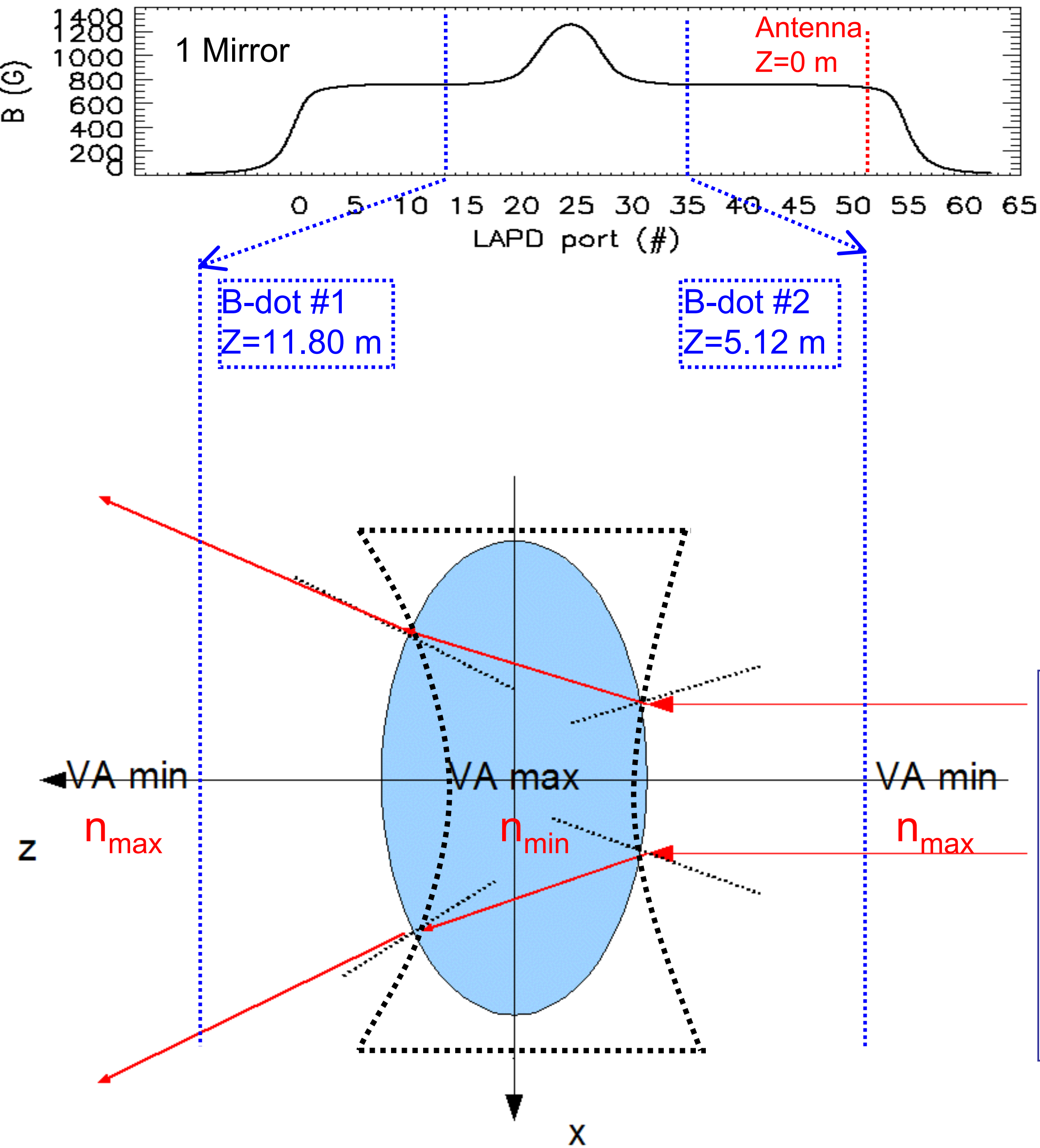

Since $v_A \propto B/\sqrt{n_i}$, $\boldsymbol{v_A}$ **maxima** correspond to the locations of $\boldsymbol{B_y}$ **maxima** and the SAW **index of refraction (n) minima.**

The mirror throat resembles a **biconvex** lens with incoming SAW travels **FASTER inside** the lens (opposite to a regular optical biconvex lens).

The SAW **index of refraction** contour at mirror throat

A virtual **Diverging** lens causing SAW to **diverge**

Multiple Mirrors Disperses Wave Pattern Radially (z=11.8 m, f=200 kHz)

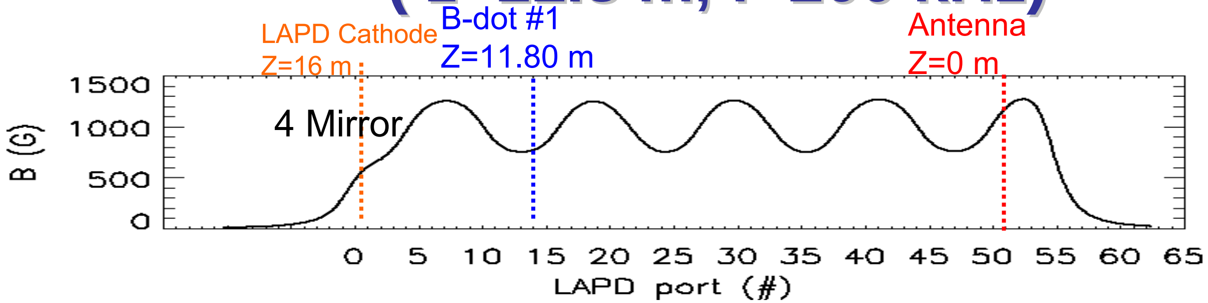

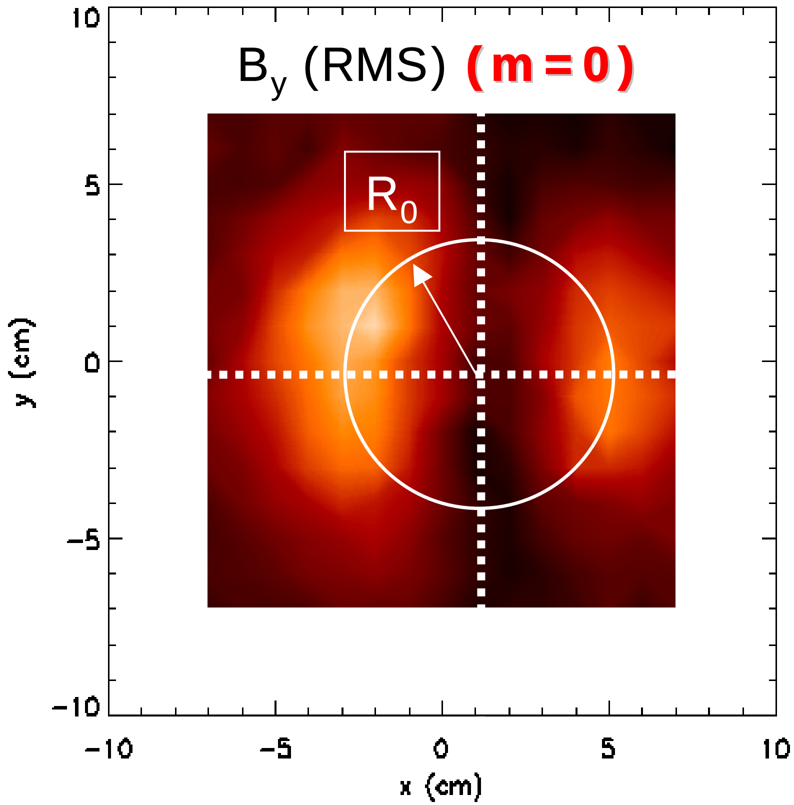

Flat Field 1.0 kG
R_0~ 3.95 cm
Cone angle~0.17º

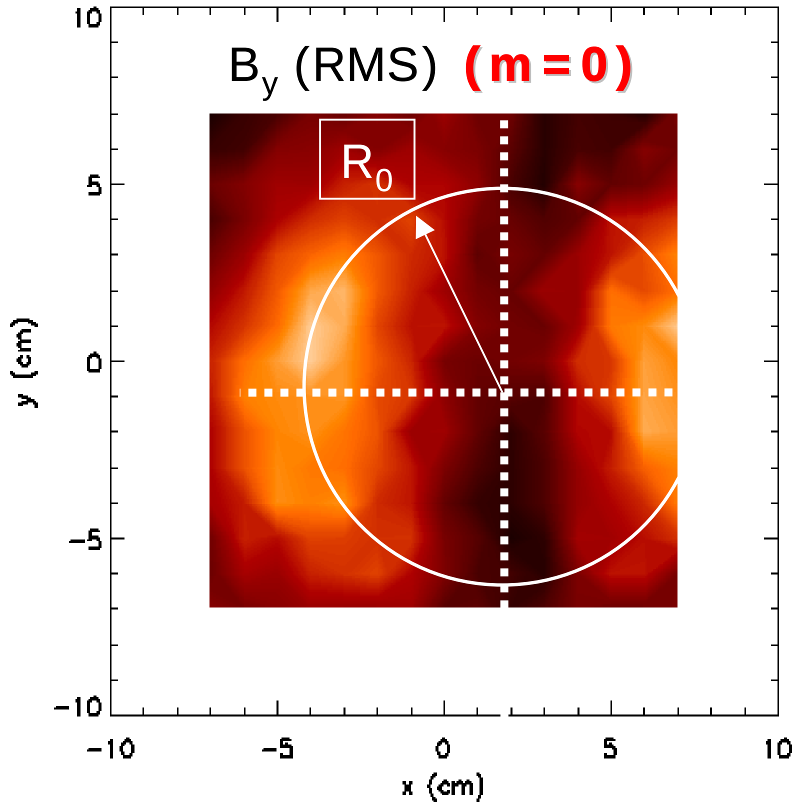

4 Mirror Configuration
R_0~ 5.50 cm
"Cone angle"~0.24º

Spectral Gap Appears with Maximum Number of Mirrors

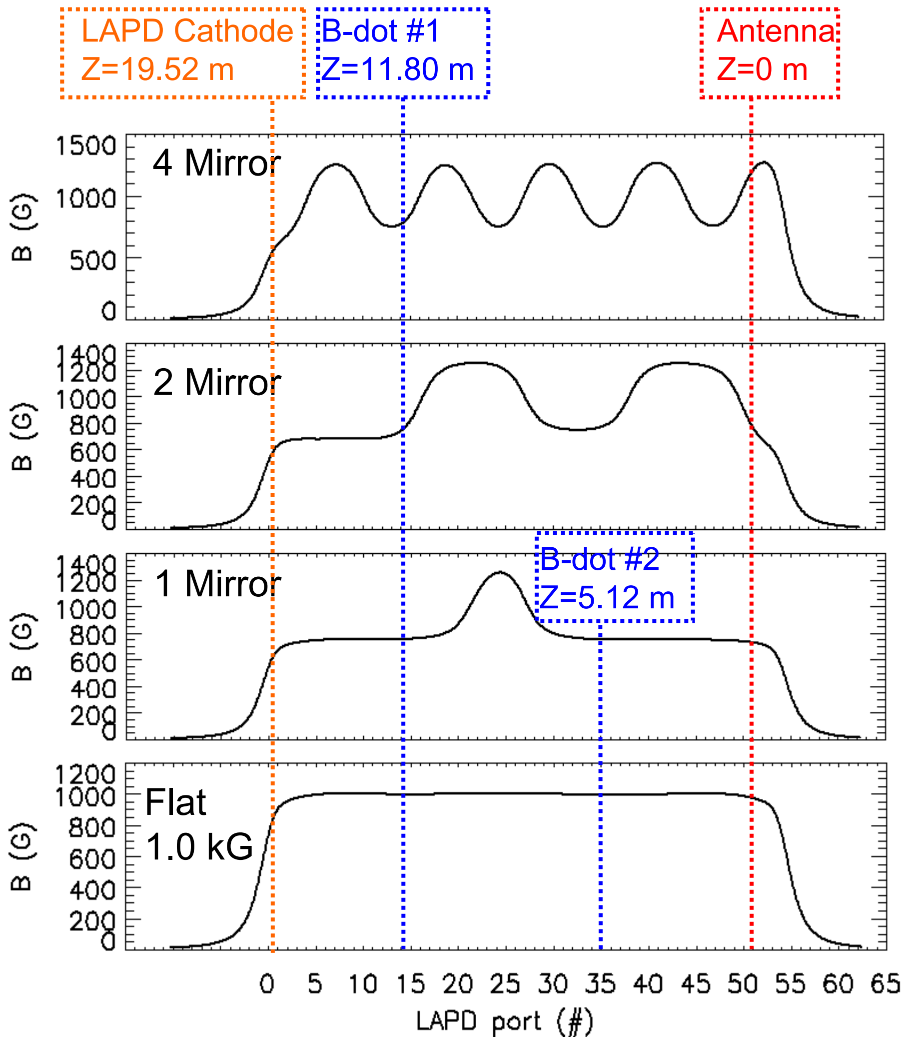

TOP: Varying number of mirror cells

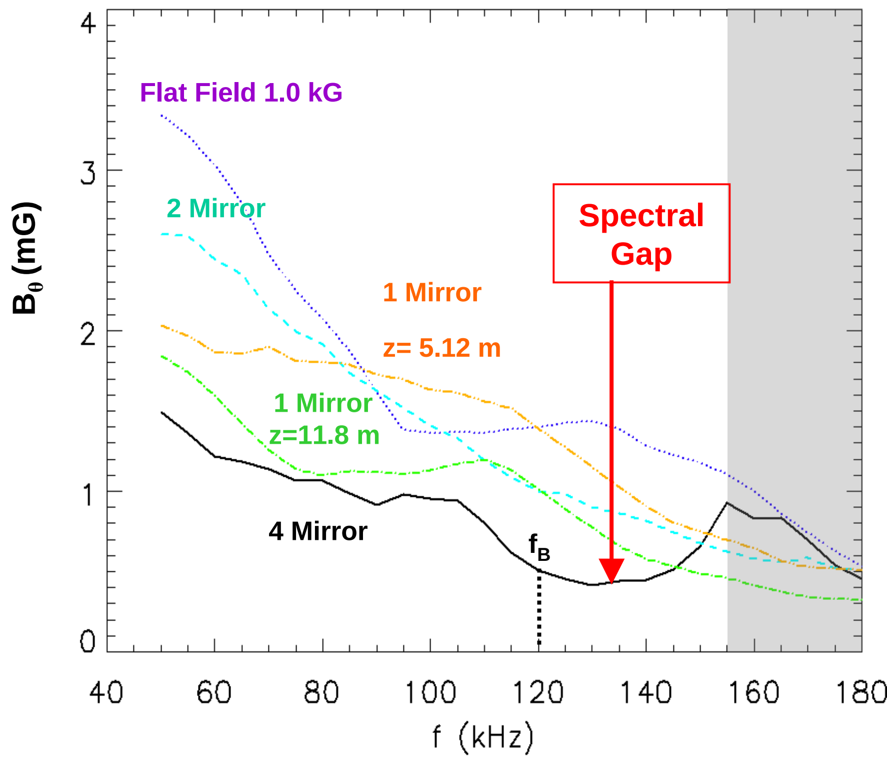

- The peak amplitude of the Alfvén-cones are plotted against frequency.
- From Bragg reflection condition

$f_B = v_{A//}/2\ \lambda_m = 120$ **kHz,** $\lambda_m = 3.6$ **m.**

- (Shaded area corresponds to large under-estimate of intensity due to truncated radial profiles.)

Gap Width is Proportional to Mirror Depth $(B_{max}-B_{min})/(B_{max}+B_{min})$

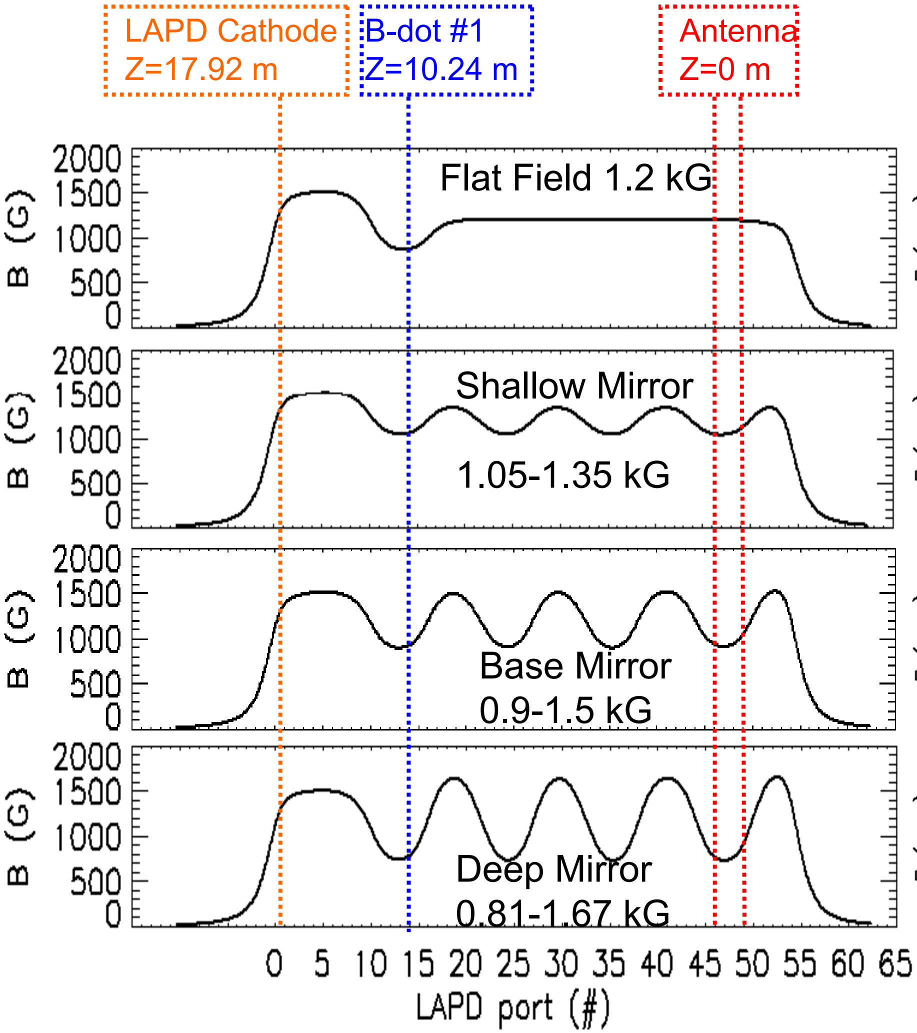

TOP: Varying mirror depth

Normalized B_θ Versus Normalized Frequency (f/f_B)

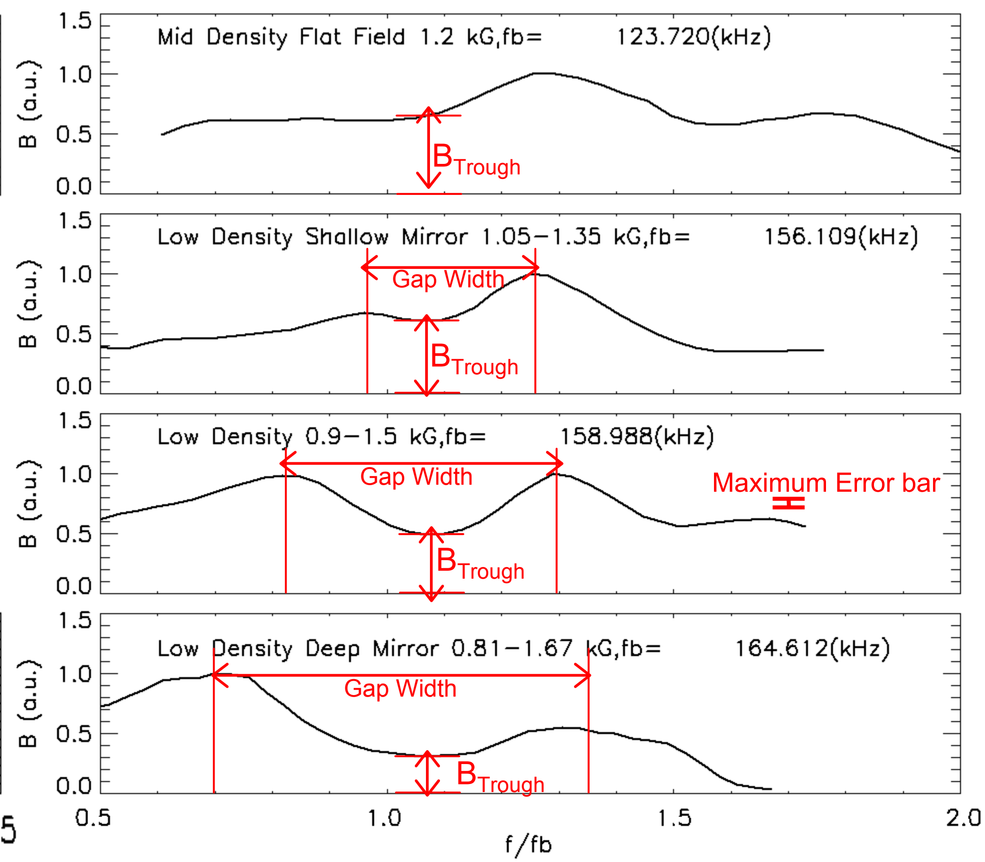

- Bragg Frequency: $f_B = v_{A//}/2\lambda_m$, $\lambda_m = 3.6$ m; $v_{A//}$ is an error source for f_B.
- Maximum error of normalized B_θ: ± 0.04 (a.u.)
- Gap width (B_{Trough}) is (inversely) proportional to mirror depth

Spectral Gap Features vs Mirror Depth $(B_{max}-B_{min})/2B_{average}$

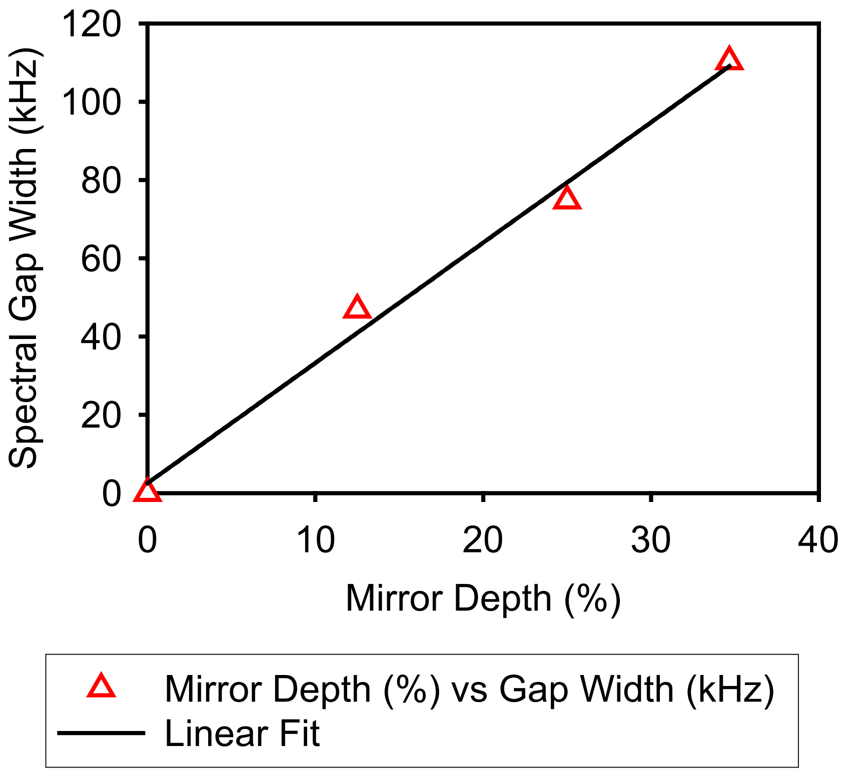

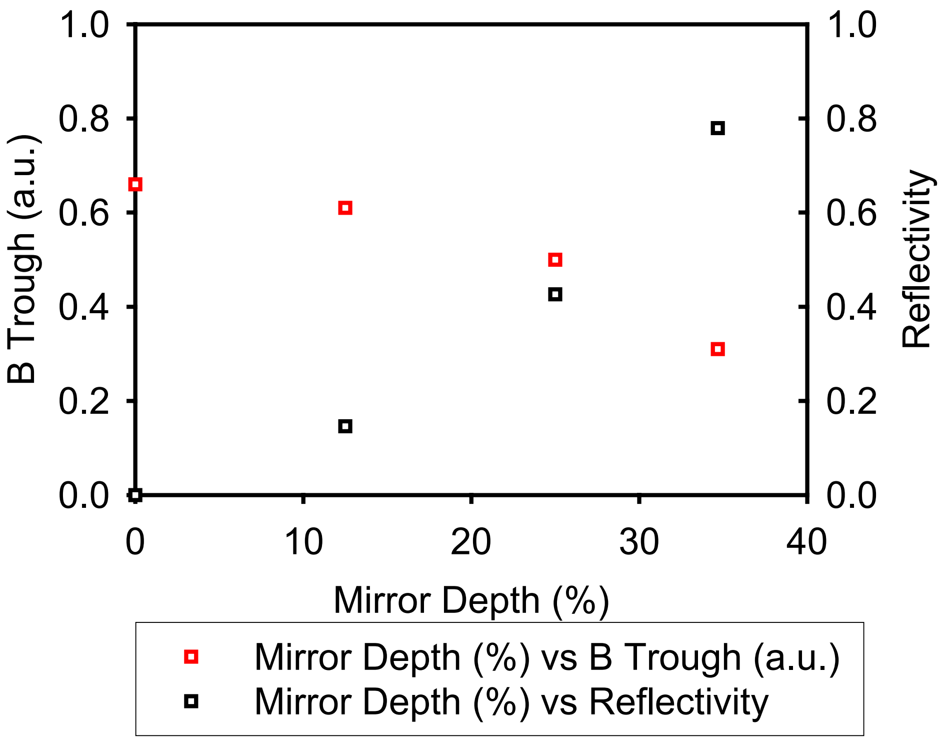

Standing Wave Mode Observed at Gap Frequency

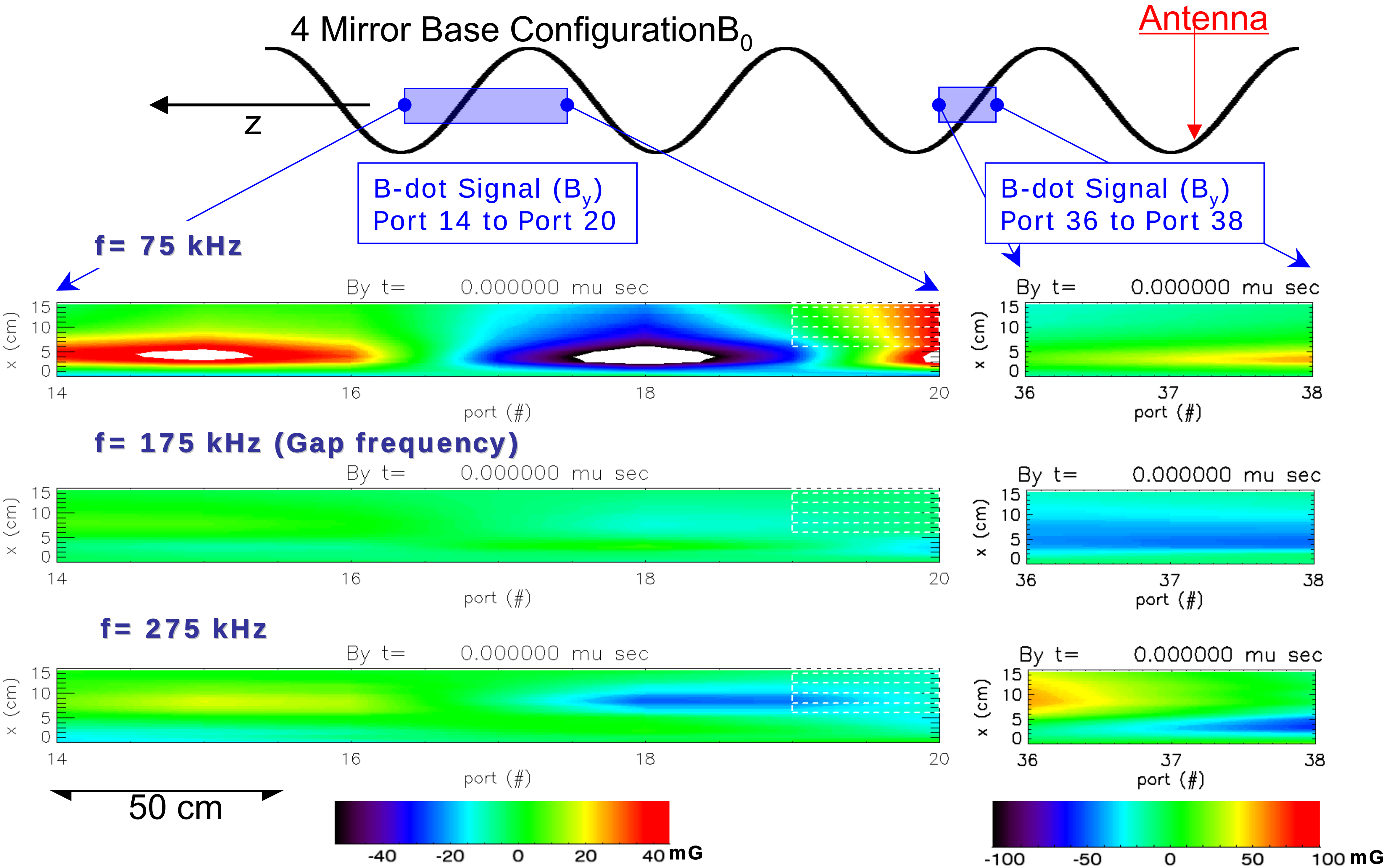

~$\lambda_m/2$ standing wavelength observed → $2\lambda_m$?

MIRROR ARRAY ALFVÉN SIMULATION
WITH EXPERIMENTAL PLASMA PARAMETERS
(UT AUSTIN, UC IRVINE)

- m=0 SAW launching and propagation is calculated by a 2D (r,z) field solver for a density profile measured from experiment
- Finite mirror array simulation shows similar spectral gap with electron-ion collision and electron Landau damping included
- Infinite mirror array simulation shows sharpest spectral gap
- The calculated gap location is found to be in good agreement with experiment

THE UNIVERSITY OF TEXAS AT AUSTIN

UCIrvine

Core Theory for Simulation

Maxwell's Equations

$$\nabla \times \mathbf{E} = \frac{i\omega}{c}\mathbf{B},$$

$$\nabla \times \mathbf{B} = -\frac{i\omega}{c}\mathbf{D} + \frac{4\pi}{c}\mathbf{j}_a,$$

where **E** and **B** are the electric and magnetic fields, **D** is the electric displacement vector, and $\mathbf{j}_a$ is the antenna current density.

$$D_\alpha = \epsilon_{\alpha\beta} E_\beta$$

where $\epsilon_{\alpha\beta}$ is the dielectric tensor. In a cold magnetized plasma, we have

$$\epsilon_{\alpha\beta} = \begin{bmatrix} \varepsilon & ig & 0 \\ -ig & \varepsilon & 0 \\ 0 & 0 & \eta \end{bmatrix}$$

where

$$\varepsilon = 1 - \sum_s \frac{\omega + i\nu_s}{\omega} \frac{\omega_{ps}^2}{(\omega + i\nu_s)^2 - \omega_{cs}^2},$$

$$g = -\sum_s \frac{\omega_{cs}}{\omega} \frac{\omega_{ps}^2}{(\omega + i\nu_s)^2 - \omega_{cs}^2},$$

$$\eta = 1 - \sum_s \frac{\omega_{ps}^2}{\omega(\omega + i\nu_s)}.$$

ν_s Includes: Electron-ion Coulomb Collision ν_{e-i}

Electron Landau Damping ν_{Landau}

Checking Simulation with Experiment Data

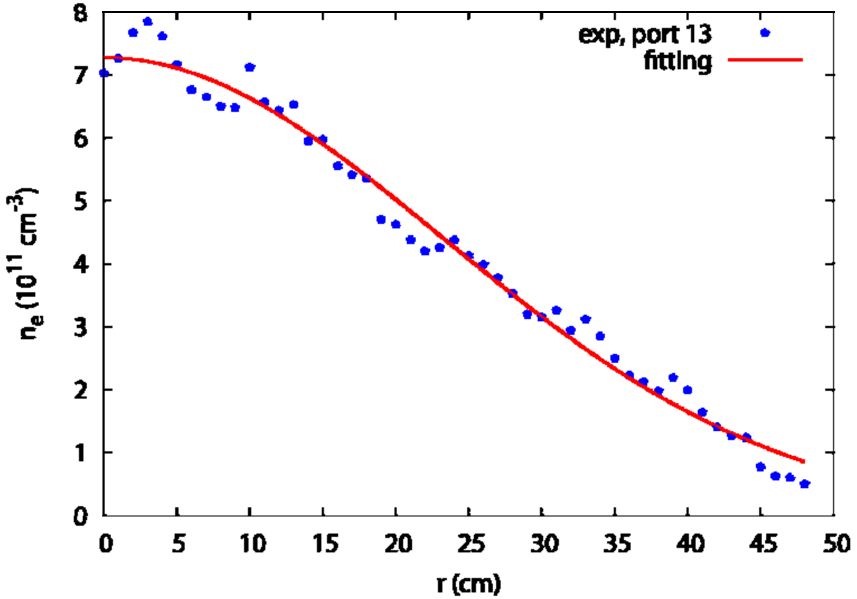

- Density radial profile theoretical fit peak $n_e \approx 7.3 \times 10^{11} cm^{-3}$
- Non-uniform radially;
- Uniform axially.

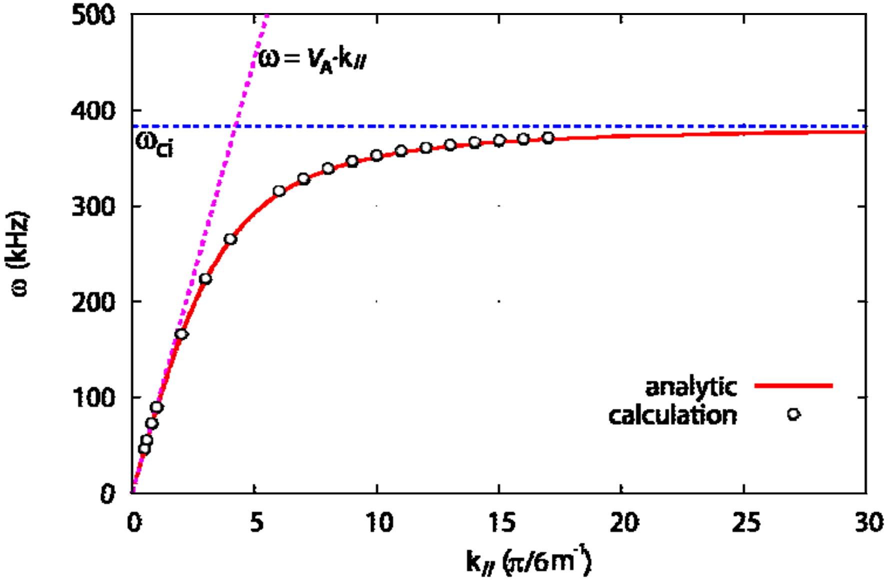

- Cold, axially-uniform plasma column with radius a=0.2m;
- Uniform B_0=1kG;

$$k_{//}^2 c^2 = \omega^2 \varepsilon - \frac{1}{2} k_\perp^2 c^2 + \sqrt{\frac{1}{4} k_\perp^4 c^4 + \varepsilon^2 \frac{\omega^6}{\omega_{ci}^2}}$$

$$(k_\perp = \pi / a)$$

Infinite Number of Mirrors —Sharp Gap

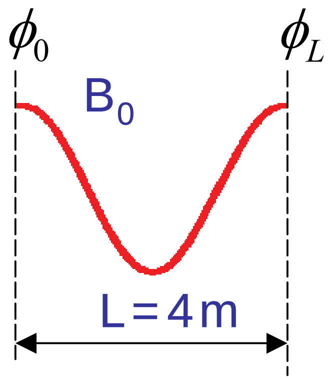

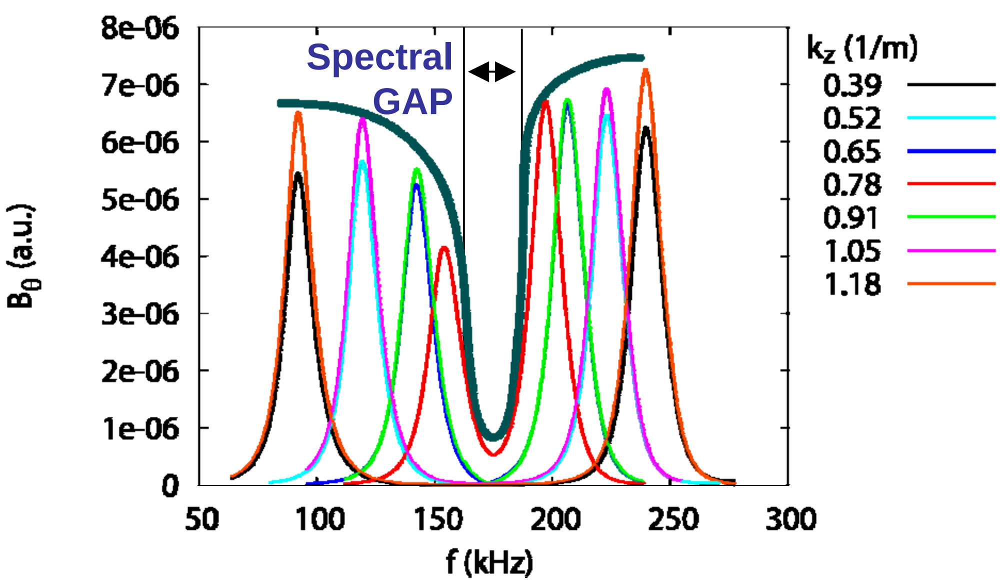

- Simulation uses one mirror with periodic boundary condition: the phase shift of electromagnetic field over the mirror is $\phi_s = \phi_L - \phi_0$
- Use measured density profile;
- Electron-ion collision frequency: $\nu_{e-i} = 2\times10^6 \quad (s^{-1})$
- m=0 modes, $k_z = \phi_s / L$
- waves of frequency between the two peaks of $\phi_s = \pi$ are significantly depressed.

Computation Setup With Magnetic Beach

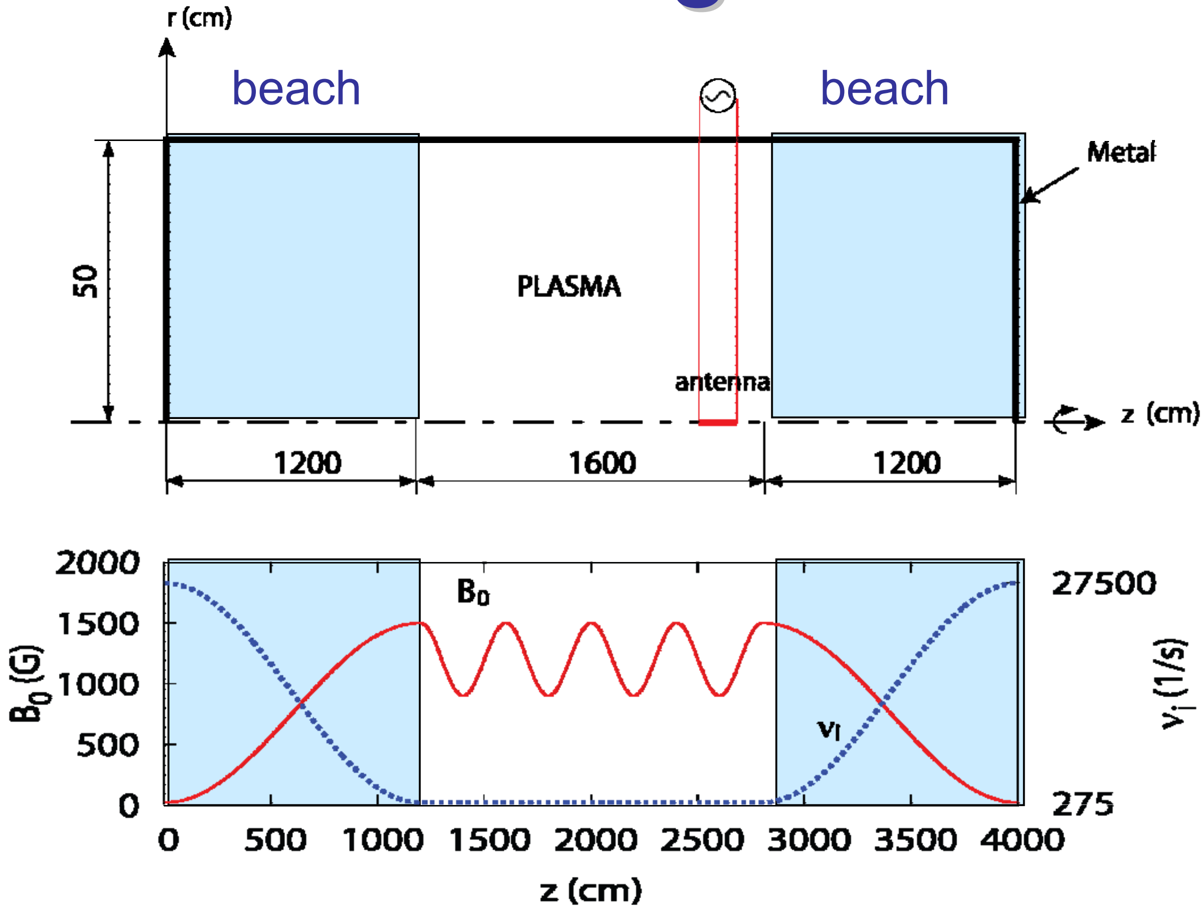

- Small Br approximation is used in the beach section so the beach section is set flatter than experiment.
- Due to limited simulation spatial grid size, the effective ion collision frequency is introduced in the beach to strengthen ion cyclotron resonance.
- Electron-ion collision frequency:

$$\nu_{e-i} = 2\times10^{6} \quad (s^{-1})$$

Virtual Frequency Scans of Wave Amplitude with Magnetic Beach

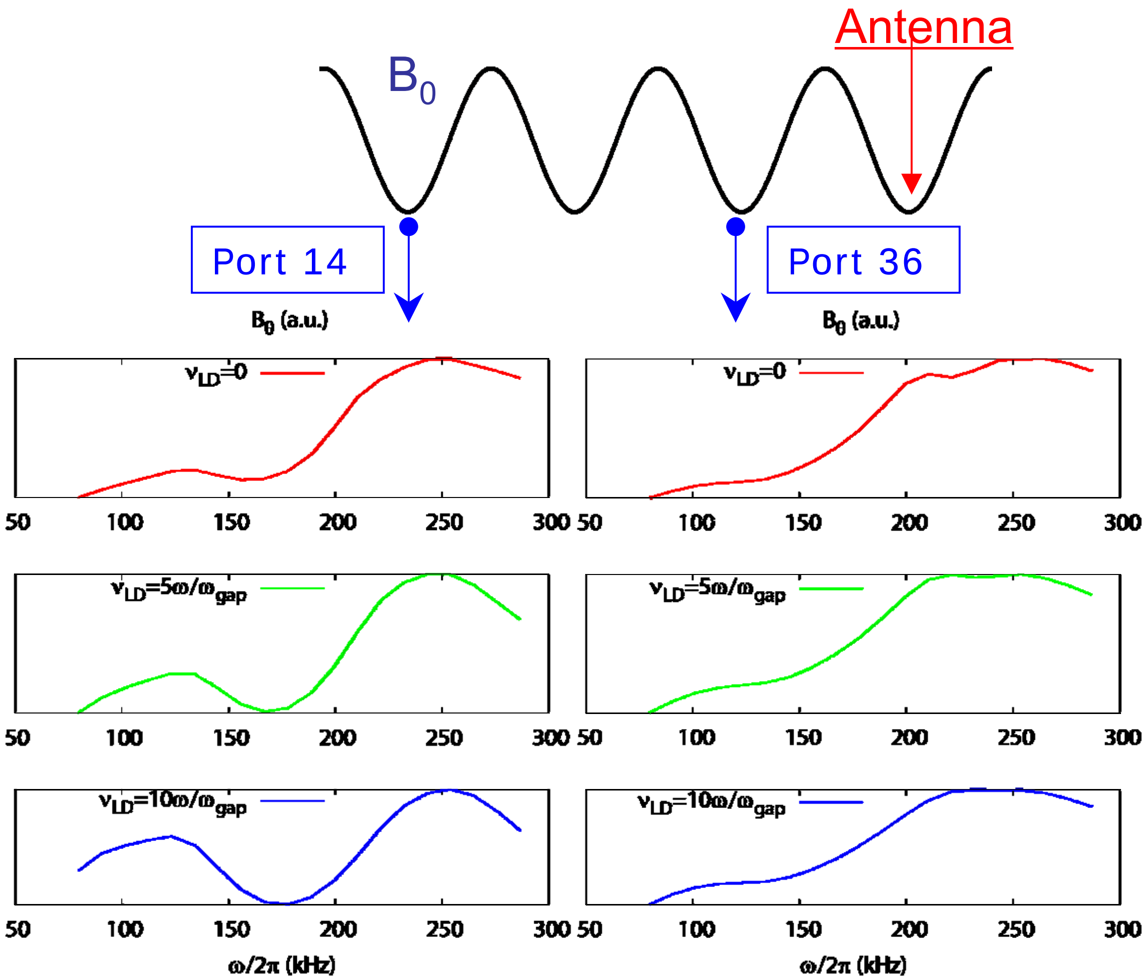

$$\nu_{e-i} = 2\times 10^{6} \quad (s^{-1})$$

- Spectral gap is evident at distant mirror away from antenna as expected.
- better antenna coupling at high frequencies.
- Wave damping due to Landau damping is more significant at high frequencies.

Increasing effective collision frequency due to Landau damping: $\nu_{\text{Landau}} \propto \omega / \omega_{Gap}$

Closer Look:
Simulation Results and Experiment Data

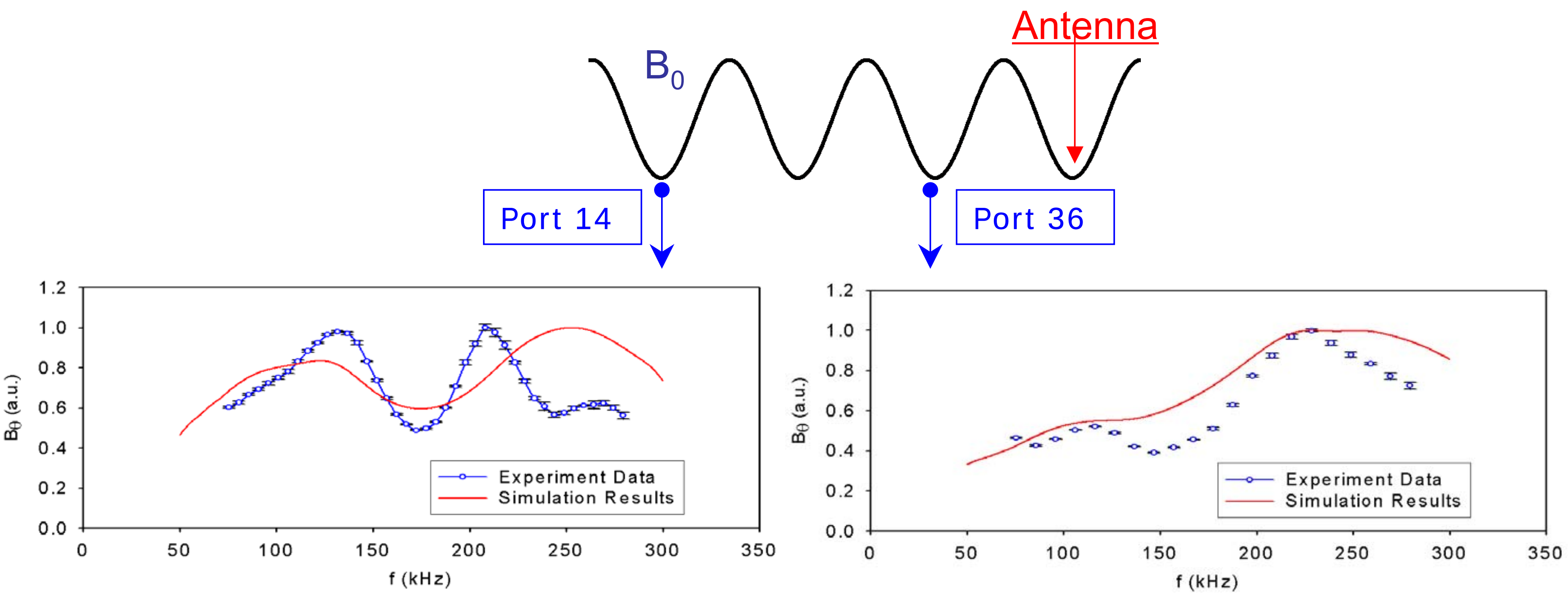

$$\nu_{e-i} = 2\times10^{6} \quad (s^{-1})$$

$$\nu_{Landau} = 10\omega/\omega_{GAP}$$

Contour Plot of Poynting Flux in z Shows Standing Wave at Gap Frequency

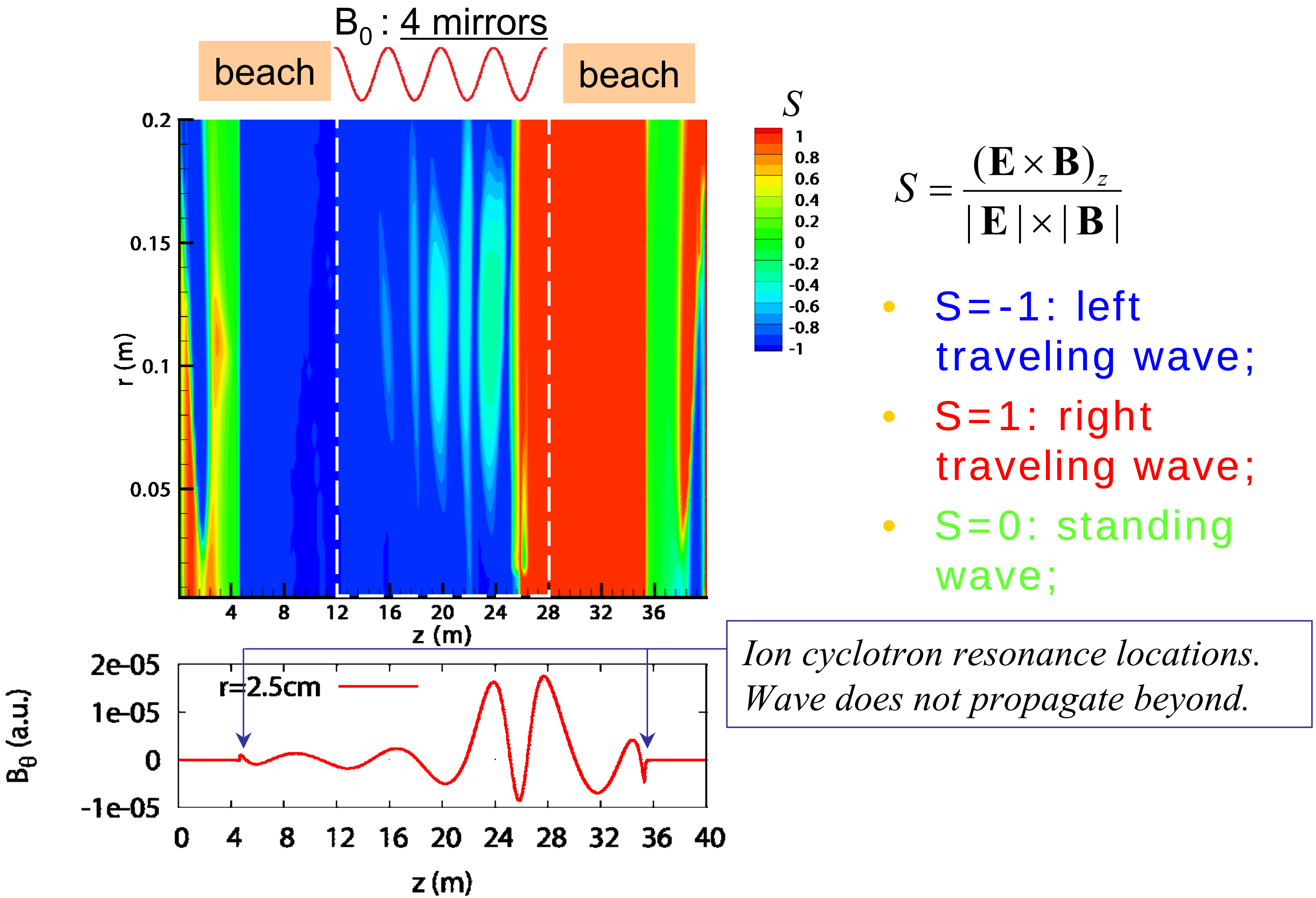

$$S = \frac{(\mathbf{E}\times\mathbf{B})_z}{|\mathbf{E}|\times|\mathbf{B}|}$$

- S=-1: left traveling wave;
- S=1: right traveling wave;
- S=0: standing wave;

CONCLUSIONS AND FUTURE WORKS

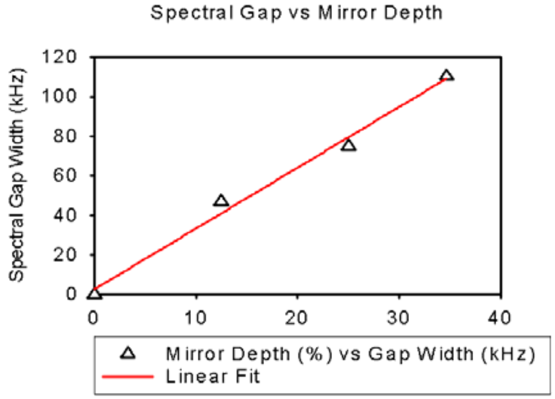

- SAW travels parallel through **Kinetic** and **Inertial** regime in the mirror array plasma;

- Multiple mirror configuration produces an observable **spectral gap** due to Bragg reflection; **Gap width** is proportional to **magnetic mirror depth**;

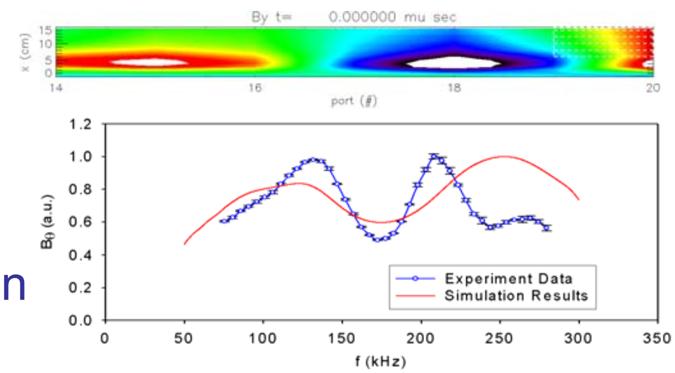

- SAW **standing wave pattern** is observed at gap frequencies, although the wavelength differs from what dispersion relation predicts;

- A **finite difference code** successfully simulates **spectral gap** features as well as wave propagation

→Acquire wavelength information for **straight field** and **single mirror cell** configuration;

→Use kinetic dispersion relation in simulation to include kinetic effect (damping, end reflection);

Thank You!

Diverging Refraction Through Single Mirror Cell Observed

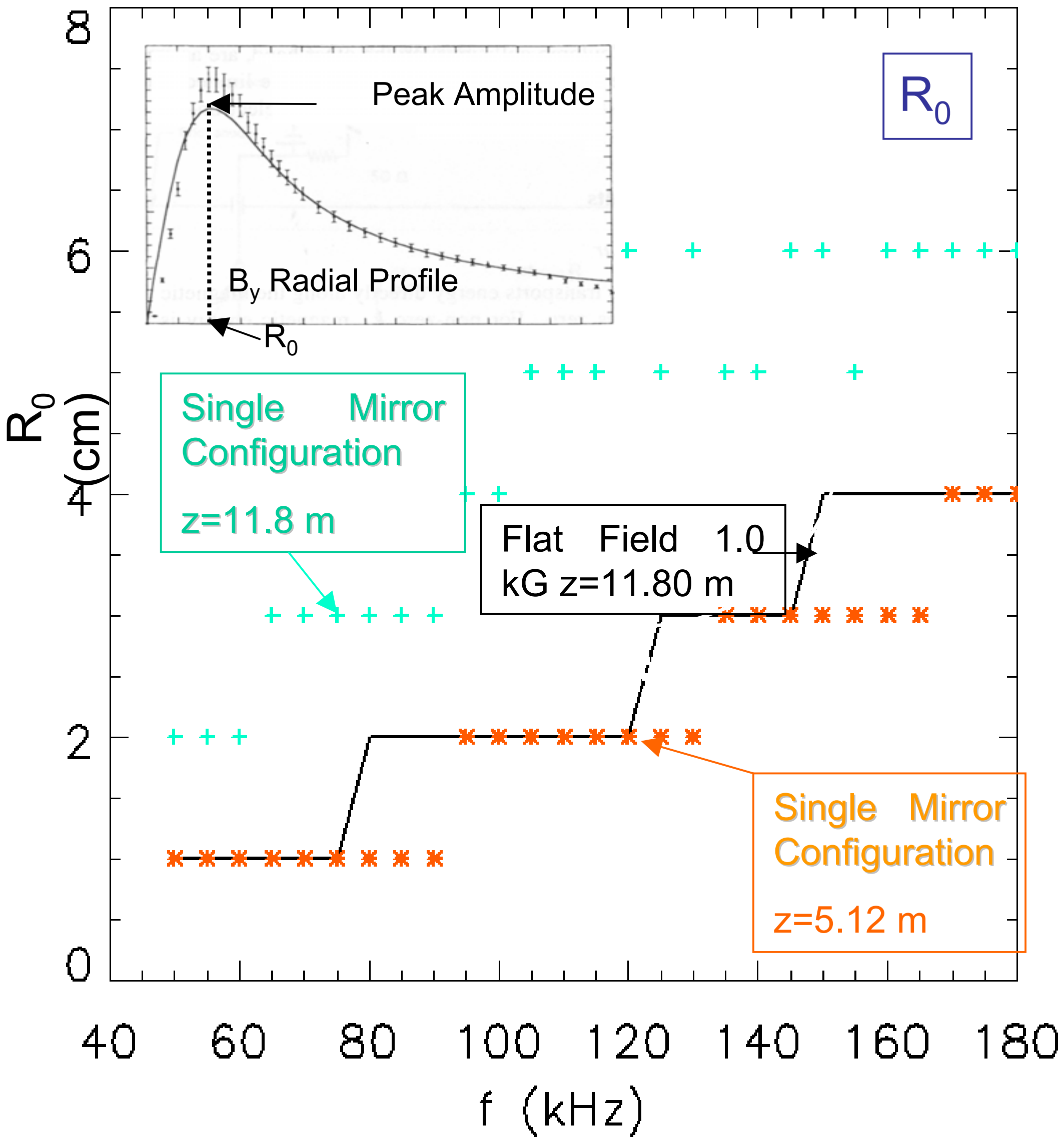

- The **peak intensity** locations of $\mathbf{B_y}$ Radial profiles are plotted versus wave frequency;
- Single mirror cell (mirror III) causes SAW to diverge **perpendicularly;**
- The radial profile **spreads out more** for **higher** wave frequencies.

Small Br Approximation

$$\frac{\partial B_{0z}}{\partial z} = f(z)$$

- $\nabla \cdot B_0 = 0 \Rightarrow \frac{1}{r}\frac{\partial}{\partial r}(rB_{0r}) + \frac{1}{r}\frac{\partial B_{0\phi}}{\partial \phi} + \frac{\partial B_{0z}}{\partial z} = 0 \Rightarrow B_{0r} = \frac{1}{2} r \frac{\partial B_{0z}}{\partial z}$
- For B_{0zmax} = 1500G, B_{0zmin} = 900G, the approximation gives $\frac{B_{0r\max}}{B_{0z\min}} \approx 0.056$ which underestimates the field lines at both ends of LAPD.
- From magnetic flux conservation:

$$\frac{B_{\min}}{B_{\max}} = \frac{r_{\max}^2}{r_{\min}^2}$$

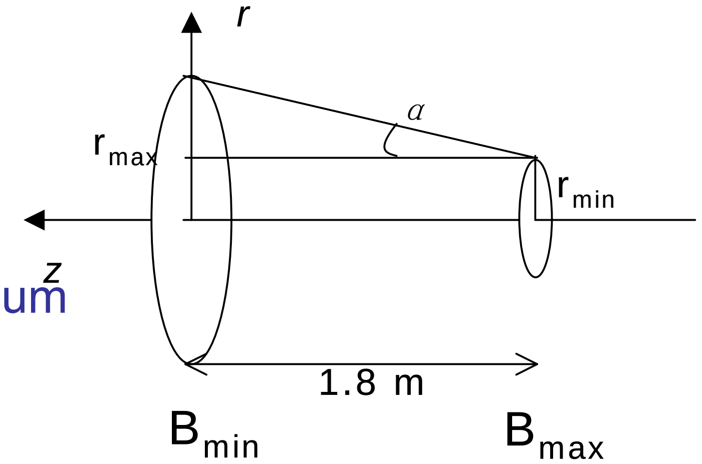

For the B-dot probe radial scan range, maximum angle of rotation:

$$\alpha_{\max} = \arctan\left(\frac{r_0 - r_1}{\lambda_m / 2}\right) \approx 1.38^{\circ}$$

Computation Setup

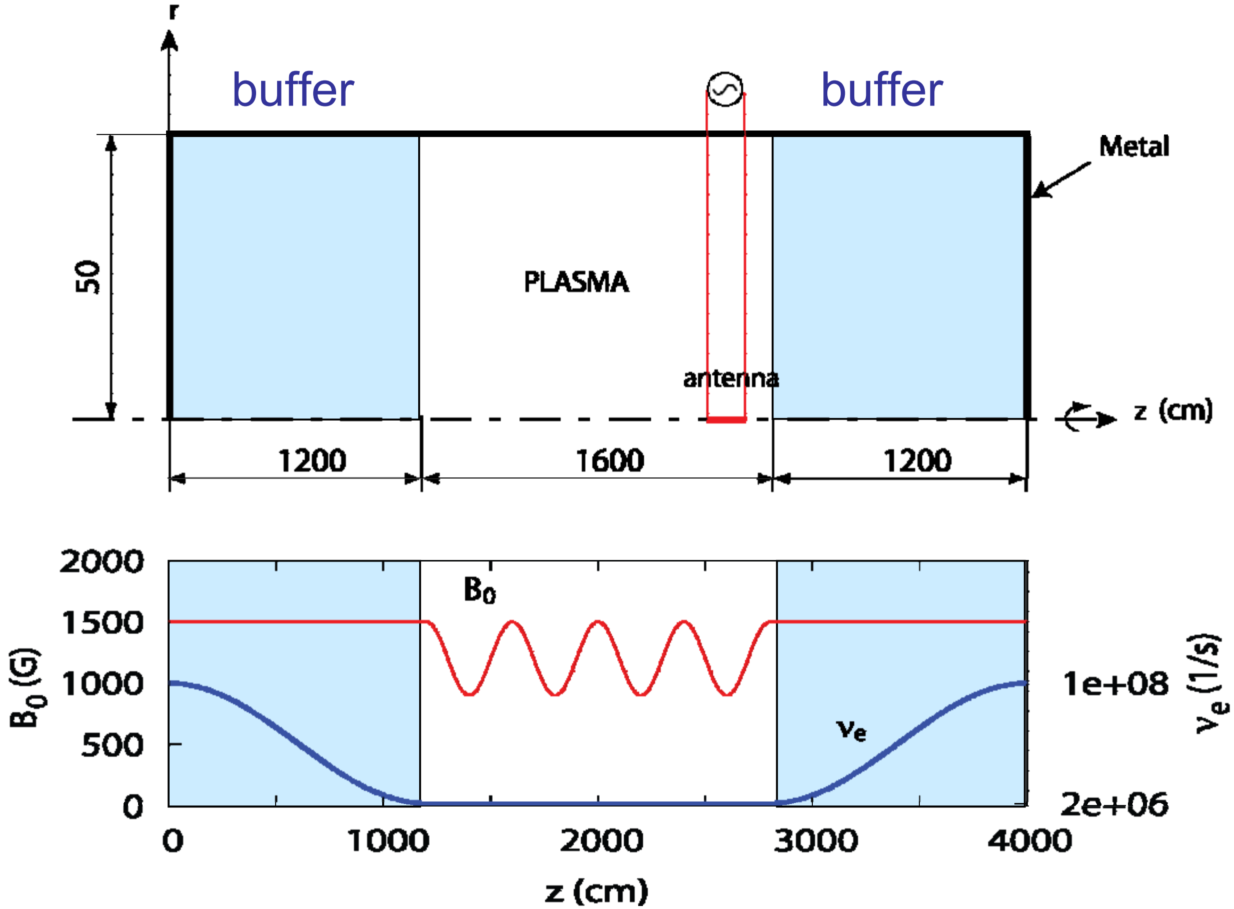

- The mirror section follows experiment, i.e. four mirrors with m. $l_m = 4$
- Use actual plasma parameters measured at LAPD
- Use a buffer section with artificially high collision frequency to absorb waves, mimicking the magnetic beach.

Frequency scan of wave amplitude

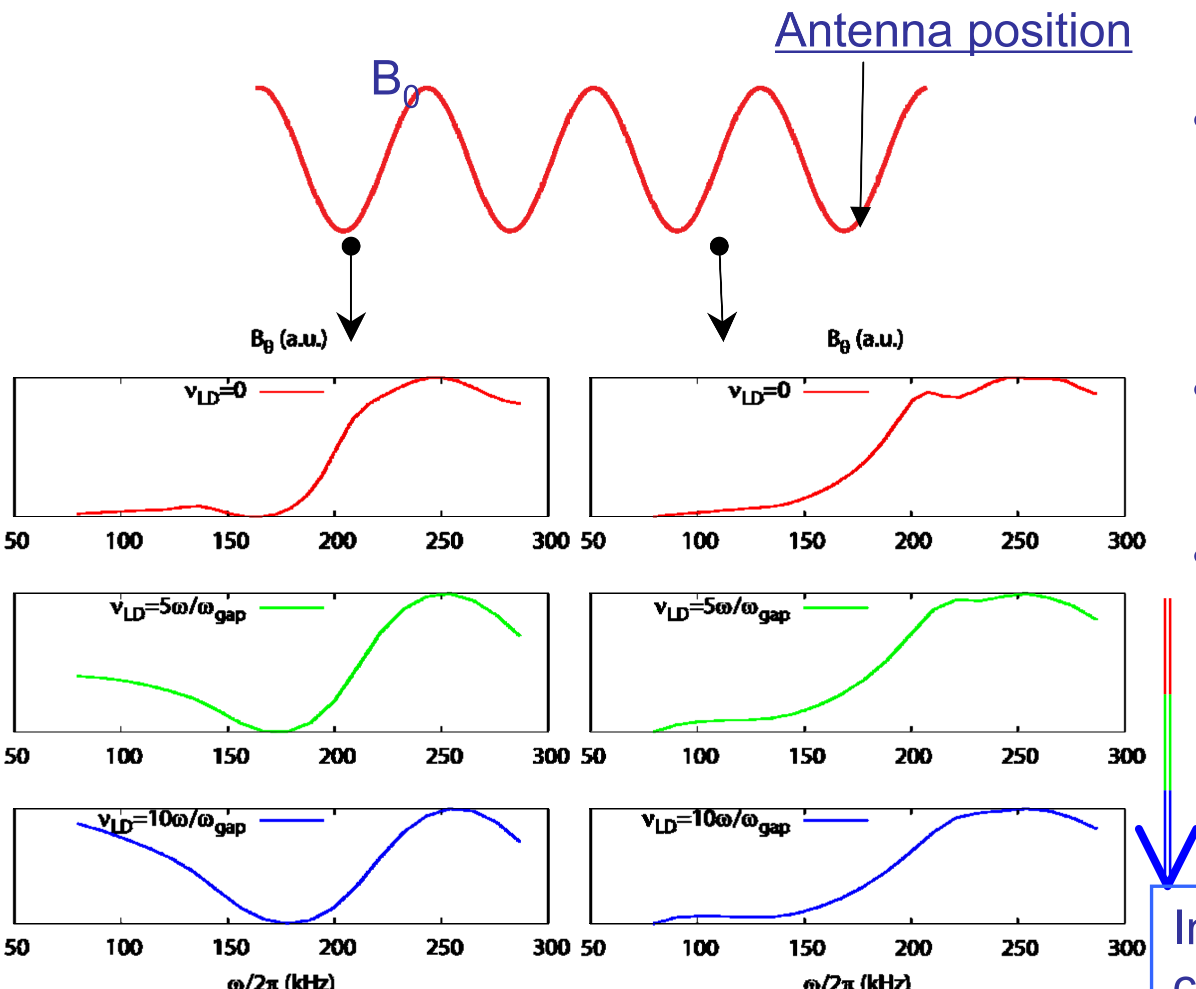

$\nu_e = 2\times10^6 \quad 1/\mathrm{s}$

- Stopping gap is evident at distant mirror away from antenna as expected.
- better antenna coupling at high frequencies.
- Wave damping due to Landau damping is more significant at high frequencies.

Increasing effective collision frequency due to Landau damping (ν_{LD}).